Olfactory regulation by dopamine and DRD2 receptor in the nose

Hai-Qian Zhou[a,1], Liu-Jing Zhuang[b,1] , Hong-Qiang Bao[c,d,1], Sheng-Ju Li[c,d], Feng-Yan Dai[a], Ping Wang[b] , Qian Li[c,d,e,2] , and Dong-Min Yin[a,2]

Olfactory behavior is important for animal survival, and olfactory dysfunction is a common feature of several diseases. Despite the identification of neural circuits and circulating hormones in olfactory regulation, the peripheral targets for olfactory modulation remain relatively unexplored. In analyzing the single-cell RNA sequencing data from mouse and human olfactory mucosa (OM), we found that the mature olfactory sensory neurons (OSNs) express high levels of dopamine D2 receptor (Drd2) rather than other dopamine receptor subtypes. The DRD2 receptor is expressed in the cilia and somata of mature OSNs, while nasal dopamine is mainly released from the sympathetic nerve terminals, which innervate the mouse OM. Intriguingly, genetic ablation of Drd2 in mature OSNs or intranasal application with DRD2 antagonist significantly increased the OSN response to odorants and enhanced the olfactory sensitivity in mice. Mechanistic studies indicated that dopamine, acting through DRD2 receptor, could inhibit odor-induced cAMP signaling of olfactory receptors. Interestingly, the local dopamine synthesis in mouse OM is down-regulated during starvation, which leads to hunger-induced olfactory enhancement. Moreover, pharmacological inhibition of local dopamine synthesis in mouse OM is sufficient to enhance olfactory abilities. Altogether, these results reveal nasal dopamine and DRD2 receptor as the potential peripheral targets for olfactory modulation.

olfactory sensitivity | dopamine | Drd2 | olfactory sensory neurons | olfactory receptor

Olfactory behavior is important for food seeking and animal survival. On the other hand, olfactory dysfunction is a common feature of several diseases such as psychiatric disorders, neurodegeneration, and COVID-19 (1–3). Interestingly, the olfactory ability can be regulated by feeding status and external environments (4, 5). Recent studies have made progress in identifying the neural circuits and circulating hormones in olfactory regulation (6–11). However, the peripheral targets modulating olfactory ability remain relatively unexplored (12).

Dopamine (DA) is a monoamine neurotransmitter (13, 14), which plays important roles in a variety of brain functions. DA is released by dopaminergic neurons in the central nervous system. In addition, DA can be released by sympathetic nerves in the peripheral tissues including the olfactory mucosa (OM) (15–18). The sympathetic innervation of rodent OM originates predominantly from the superior cervical ganglion (SCG) (17). Tyrosine hydroxylase (TH) is the rate-limiting enzyme for DA synthesis (19). Intriguingly, the Th mRNA is locally translated in the sympathetic nerve axons, which facilitates local DA synthesis (20, 21).

There are two types of DA receptors based on sequence homology and function: The excitatory D1-like receptors (DRD1 and DRD5) and inhibitory D2-like receptors (DRD2–DRD4) (22). Activation of DRD2, a $G\alpha_{i/o}$-coupled receptor, can reduce the intracellular levels of cyclic adenosine monophosphate (cAMP). Drd2 is associated with several neuropsychiatric diseases and is the target of some antipsychotic drugs (23–28). In the central nervous system including the olfactory bulb (OB), DA-DRD2 signaling plays important roles in regulating synaptic transmission and plasticity (29–33). However, the function and regulation of DA-DRD2 signaling in the peripheral tissues are relatively less understood.

Here we show that DRD2 is expressed in the cilia and somata of mature olfactory sensory neurons (OSNs) in mice. We provide evidence that DA-DRD2 signaling has a tonic inhibition on OSN activity and olfactory function in mice. Intriguingly, hunger greatly reduces the N4-acetylcytidine (ac[4]C) modification of Th mRNA and local DA synthesis in mouse OM, which causes the olfactory enhancement during starvation. We further show that inhibition of local DA synthesis or DRD2 receptor in mouse OM recapitulates enhanced olfactory abilities during starvation. Collectively, these results reveal nasal DA and DRD2 receptor as the potential peripheral targets for olfactory regulation.

Significance

Despite the identification of neural circuits and circulating hormones in olfactory regulation, the peripheral targets for olfactory modulation remain relatively unexplored. Here we show that dopamine D2 receptor (DRD2) is expressed in the cilia and somata of mature olfactory sensory neurons (OSNs), while nasal dopamine (DA) is mainly released from the sympathetic nerve terminals, which innervate the mouse olfactory mucosa (OM). We further demonstrate that DA-DRD2 signaling in the nose plays important roles in regulating olfactory function using genetic and pharmacological approaches. Moreover, the local DA synthesis in mouse OM is reduced during hunger, which contributes to starvation-induced olfactory enhancement. Altogether, we demonstrate that nasal DA and DRD2 receptor can serve as the potential peripheral targets for olfactory modulation.

Results

Expression of DRD2 in the Cilia and Somata of Mature OSNs from Mice.

Analysis of our previous single-cell RNA sequencing data from mouse OM revealed that the mature OSNs expressed Drd2 receptor, but not other DA receptor subtypes (34). To further investigate the cellular expression pattern of Drd2 in mouse OM, we generated Drd2-reporter mice (35) that express tdTomato in Drd2-positive cells (Fig. 1A and *SI Appendix,* Fig. S1 *A* and *B*). Most cells expressing tdTomato also express OMP (olfactory marker protein, a typical marker for mature OSNs, OMP$^+$/Drd2$^+$ = 92.94 ± 0.7344%, n = 12 slices from three mice), which indicates that most Drd2-positive cells in mouse OM are mature OSNs (Fig. 1B and *SI Appendix,* Fig. S1C). On the other hand, the majority of mature OSNs in mouse OM express Drd2 (Drd2$^+$/OMP$^+$ = 72.34 ± 3.123%, n = 12 slices from three mice) (Fig. 1B and *SI Appendix,* Fig. S1C). The distinct OSN subpopulations expressing TAAR5, a trace amine-associated receptor or MOR42-3/Olfr544, an odorant receptor, are also Drd2-positive (Fig. 1 *C* and *D* and *SI Appendix,* Fig. S1 *D* and *E*). By contrast, we did not observe Drd1 expression in the mature OSNs from Drd1-reporter mice (*SI Appendix,* Fig. S1F), which is consistent with the previous study (36).

To explore the subcellular localization of DRD2 proteins in mouse OM, we performed immunostaining of DRD2 in the OM from adult wild-type (WT) and Drd2$^{-/-}$ mice. As shown in Fig. 1E, DRD2 is expressed in the somata but not the nucleus of mature OSNs. In addition, DRD2 is partially colocalized with acetylated-tubulin (Ac-tubulin, a protein marker for cilia), which suggests that DRD2 is trafficked into the cilia

of mature OSNs. Note that the immunofluorescent signal of DRD2 is absent in the OM from Drd2$^{-/-}$ mice (37) (Fig. 1E), validating the specificity of the DRD2 antibody for immunostaining (38). Intriguingly, the single-cell RNA sequencing of human OM also indicated that mature OSNs express Drd2 rather than other DA receptor subtypes (39). Moreover, the expression levels of Drd2 in other types of cells are much lower than those in the mature OSNs from human OM (Fig. 1F). Altogether, these results indicate that the expression of Drd2 in mature OSNs is conserved between mouse and human.

Enhanced Olfactory Sensitivity by Genetic Ablation of Drd2 in Mature OSNs.

Since DRD2 is a Gα$_{i/o}$-coupled receptor (22), we speculate that genetic deletion of Drd2 in mature OSNs would lead to the disinhibition of mature OSNs and increase of olfactory abilities. To test this hypothesis, we generated Drd2 conditional knockout mice by crossing Omp$^{Cre/+}$ mice (40) with Drd2$^{f/f}$ mice (41). The resulting Omp$^{Cre/+}$; Drd2$^{f/f}$ mice were named Omp-Drd2$^{-/-}$ mice, where Drd2 is selectively deleted in mature OSNs (Fig. 2A). To avoid the potential effects of Cre insertion in the Omp gene, the Omp$^{Cre/+}$ mice were used as controls in the following experiments. The DRD2 proteins were significantly reduced in the OM but not in the OB from Omp-Drd2$^{-/-}$ mice, compared with controls (Fig. 2 *B* and *C*). Genetic ablation of Drd2 in mature OSNs did not alter the number of mature OSNs or their projections to the OB (*SI Appendix,* Fig. S2). The body weight and locomotion were similar between control and Omp-Drd2$^{-/-}$ mice (*SI Appendix,* Fig. S3 *A–D*). The time to find the visible food was also similar between control and Omp-Drd2$^{-/-}$ mice (*SI Appendix,* Fig. S3 *E* and *F*).
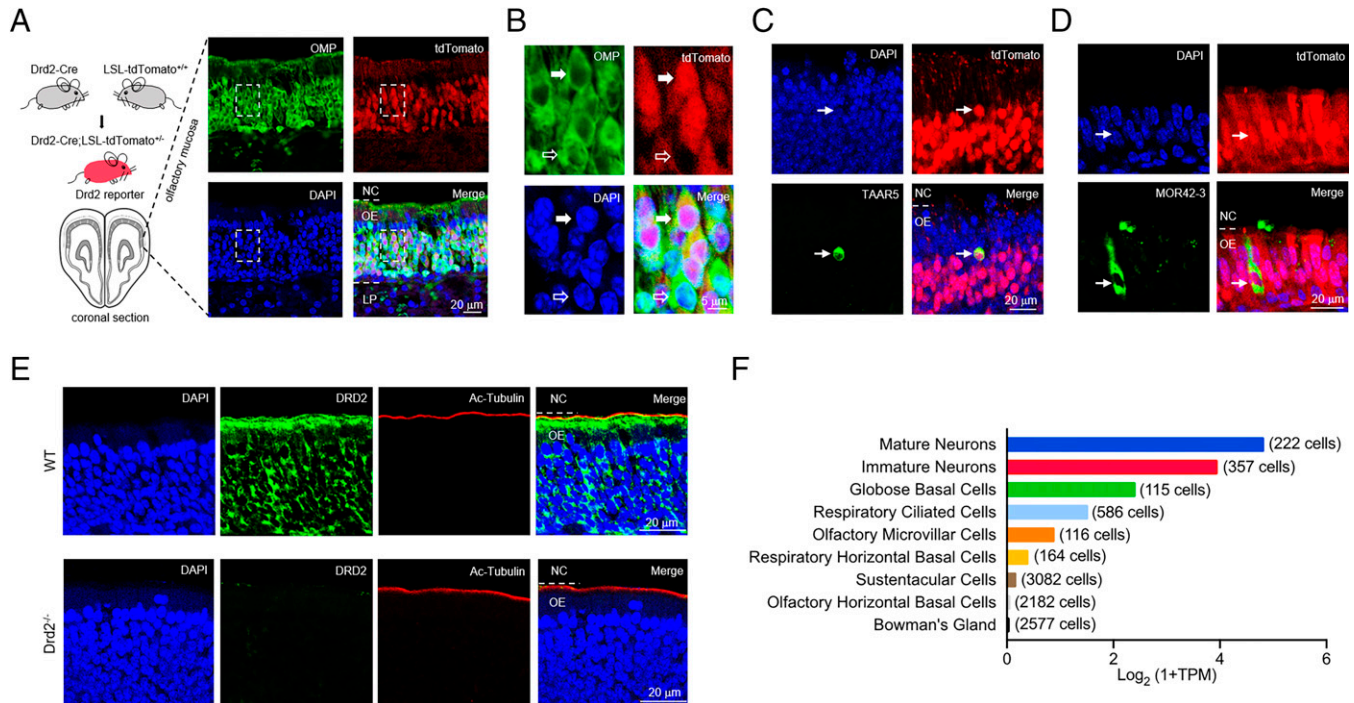

Fig. 1. Expression of DRD2 in the cilia and somata of mature OSNs in mice. (A) Drd2 reporter mice revealed expression of Drd2 in mature OSNs. The Drd2 reporter mice (Drd2-Cre; LSL-tdTomato$^{+/-}$) were generated by crossing Drd2-Cre mice with loxp-stop-loxp-tdTomato (LSL-tdTomato$^{+/+}$) reporter mice. The OM slices from Drd2 reporter mice were immunostained with antibody against OMP, a marker for mature OSNs. NC, nasal cavity; OE, olfactory epithelium; LP, lamina propria. (Scale bar, 20 μm.) (B) Enlarged images form the rectangle in A. The solid arrow indicates a mature OSN expressing Drd2. The empty arrow indicates a mature OSN not expressing Drd2. (Scale bar, 5 μm.) (C) Drd2-positive OSN expresses TAAR5. (Scale bar, 20 μm.) (D) Drd2-positive OSN also expresses MOR42-3. (Scale bar, 20 μm.) (E) Immunostaining of DRD2 and acetylated-tubulin (Ac-tubulin) in the OM from WT (*Top*) and Drd2$^{-/-}$ (*Bottom*) mice. Four independent experiments were repeated to get similar results. (Scale bar, 20 μm.) (F) Gene expression levels (TPM, transcripts per million) of *Drd2* receptor in the major types of cells from human OM. The x axis indicates the value of log$_2$ (1+ TPM). The y axis indicates different types of cells in the OM. The numbers of each type of cells are indicated in the bracket.
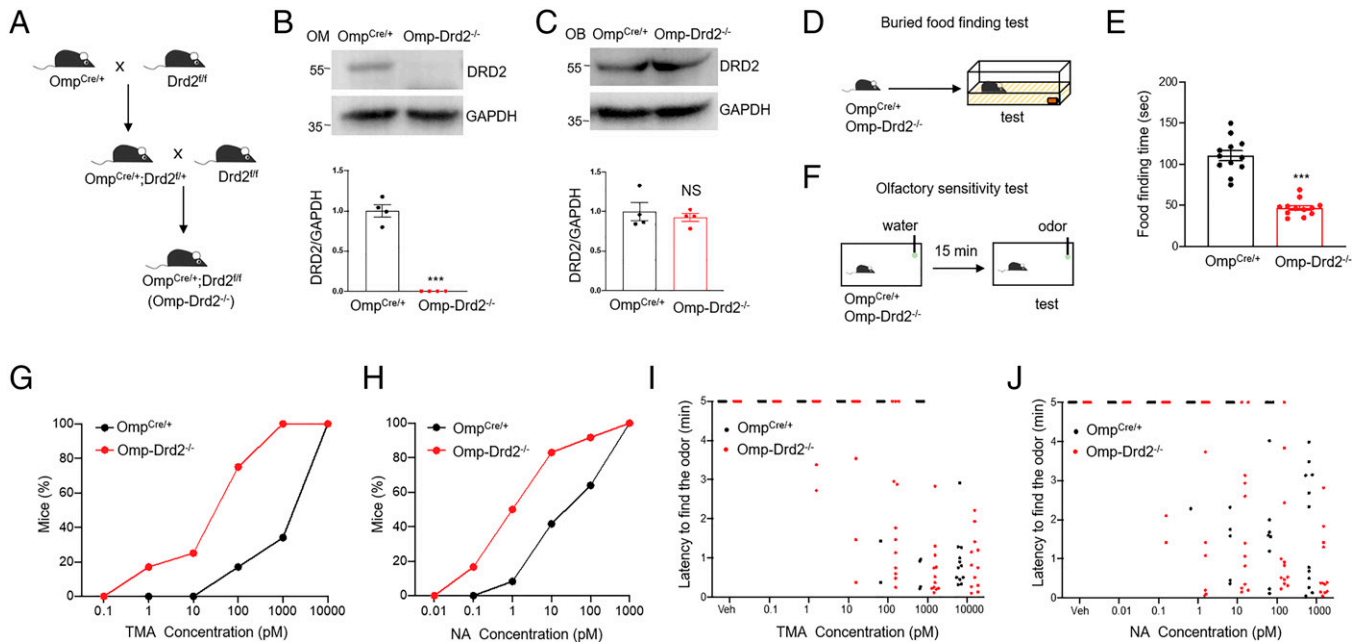
Fig. 2. Genetic ablation of Drd2 from mature OSNs increases olfactory abilities. (A) The breeding strategy to generate Omp-Drd2$^{-/-}$ mice. (B) Reduction of DRD2 protein levels in the OM from Omp-Drd2$^{-/-}$ mice. *Top*, representative blots. The homogenates of OM from control (Omp$^{Cre/+}$) and Omp-Drd2$^{-/-}$ mice were subjected to Western blot and probed with the indicated antibodies. *Bottom*, quantification of DRD2/GAPDH. The data were normalized to the control group. ***$P < 0.0001$, two-sided t test, $n = 4$ mice per group. Data are presented as mean values ± SEM. (C) No change of DRD2 protein levels in the OB from Omp-Drd2$^{-/-}$ mice. *Top*, representative blots. The homogenates of OB from control (Omp$^{Cre/+}$) and Omp-Drd2$^{-/-}$ mice were subjected to Western blot and probed with the indicated antibodies. *Bottom*, quantification of DRD2/GAPDH. The data are normalized to the control group. NS, not significant ($P = 0.5608$), two-sided t test, $n = 4$ mice per group. Data are presented as mean values ± SEM. (D) Experimental design. The control (Omp$^{Cre/+}$) and Omp-Drd2$^{-/-}$ mice that had normal access to food were subjected to the buried food finding test. (E) The Omp-Drd2$^{-/-}$ mice showed better olfactory abilities than controls. The time to find the buried food was quantified. ***$P < 0.0001$, two-sided t test, $n = 12$ mice per group. (F) Experimental design. The control (Omp$^{Cre/+}$) and Omp-Drd2$^{-/-}$ mice were habituated in the testing cages for 15 min and then tested for the olfactory sensitivity to TMA and NA. (G and H) Olfactory sensitivity to TMA (G) and NA (H) is increased in Omp-Drd2$^{-/-}$ mice, compared with controls. Shown are the sniffing curves of two groups of mice. The x axis represents different concentrations of TMA or NA. The y axis indicates the percentage of the mice that found the odor source within 5 min. $n = 12$ mice per group. (I, J) Latency to find TMA (I) and NA (J) is shortened in Omp-Drd2$^{-/-}$ mice, compared with controls. Shown are the times taken to find the odor source TMA (I) and NA (J) in two groups of mice. Each point depicts a single individual. Mice that failed to find the odorants in 5 min were plotted at 5. The x axis represents different concentrations of TMA or NA. The y axis indicates the latency to find the odor source. $P < 0.0001$ for both TMA and NA, the Scherier–Ray–Hare test, $n = 12$ mice per group.

Next, the Omp-Drd2$^{-/-}$ mice and their controls were subjected to the buried food finding test that is commonly used to study olfactory abilities (42) (Fig. 2D). The time to find the buried food was significantly less in Omp-Drd2$^{-/-}$ mice compared with their controls (Fig. 2E), which suggests that genetic ablation of Drd2 in mature OSNs may increase olfactory abilities. To solidify this notion, we performed an olfactory sensitivity test in Omp-Drd2$^{-/-}$ mice and their controls (Fig. 2F). Here we analyzed the olfactory sensitivity to trimethylamine (TMA) and nonanedioic acid (NA), the ligands for TAAR5 and MOR42-3, respectively (43, 44). Recall that the mature OSNs expressing TAAR5 or MOR42-3 also express Drd2 (Fig. 1 C and D). The sniffing curves toward different concentrations of TMA and NA shifted leftward in Omp-Drd2$^{-/-}$ mice, compared with controls (Fig. 2 G and H). A total of 75% (8/12) of the Omp-Drd2$^{-/-}$ mice could find 100 pM TMA in 5 min, whereas only 16.7% (2/12) of control mice could (Fig. 2G). Half (6/12) of the Omp-Drd2$^{-/-}$ mice could find 1 pM NA in 5 min, whereas only 8.3% (1/12) of control mice could (Fig. 2H). Likewise, the latency to find the odor source of TMA and NA was significantly decreased in Omp-Drd2$^{-/-}$ mice, compared with controls (Fig. 2 I and J). Taken together, these results demonstrate that genetic deletion of Drd2 in mature OSNs increases the olfactory sensitivity in mice.

Increase of Olfactory Abilities by Intranasal Inhibition of DRD2. Next, we investigated whether acute inhibition of DRD2 in the nose could affect olfactory abilities in WT mice. To this end, we treated mice with eticlopride (Eti, 0.1 mg/kg)

(45), a DRD2 antagonist or vehicle through intranasal delivery 3 min before the buried food finding test (Fig. 3A). Intriguingly, intranasal application with Eti significantly reduced the time to find the buried food in WT mice (Fig. 3B). By contrast, intranasal delivery of Eti did not affect the time to find the buried food in Omp-Drd2$^{-/-}$ mice (*SI Appendix,* Fig. S4 A and B), which indicates that intranasal application with Eti regulates olfactory ability mainly through DRD2 in the mature OSNs. Intranasal delivery of Eti did not affect the locomotion or the time to find the visible food in WT mice (*SI Appendix,* Fig. S4 C–G), excluding any nonolfactory effects. Altogether, these results suggest that acute inhibition of DRD2 in the nose can enhance the olfactory abilities in mice.

We further studied whether acute inhibition of DRD2 in the nose of WT mice could increase the olfactory sensitivity to TMA and NA, as we did for the Omp-Drd2$^{-/-}$ mice (Fig. 2 G–J). We performed intranasal delivery of Eti or vehicle 3 min before the olfactory sensitivity tests (Fig. 3C). The sniffing curves toward different concentrations of TMA and NA shifted leftward in Eti-treated mice, compared with vehicle-treated mice. Half (6/12) of the Eti-treated mice could find 300 pM TMA in 5 min, whereas only 8.3% (1/12) of control mice could (Fig. 3D). A total of 75% (9/12) of Eti-treated mice could find 10 pM NA in 5 min, whereas only 41.6% (5/12) of control mice could (Fig. 3E). Likewise, the latency to find the odor source of TMA and NA was significantly reduced in Eti-treated mice, compared with vehicle-treated mice (Fig. 3 F and G). All these results demonstrate that intranasal inhibition of DRD2 can increase the olfactory sensitivity in mice.
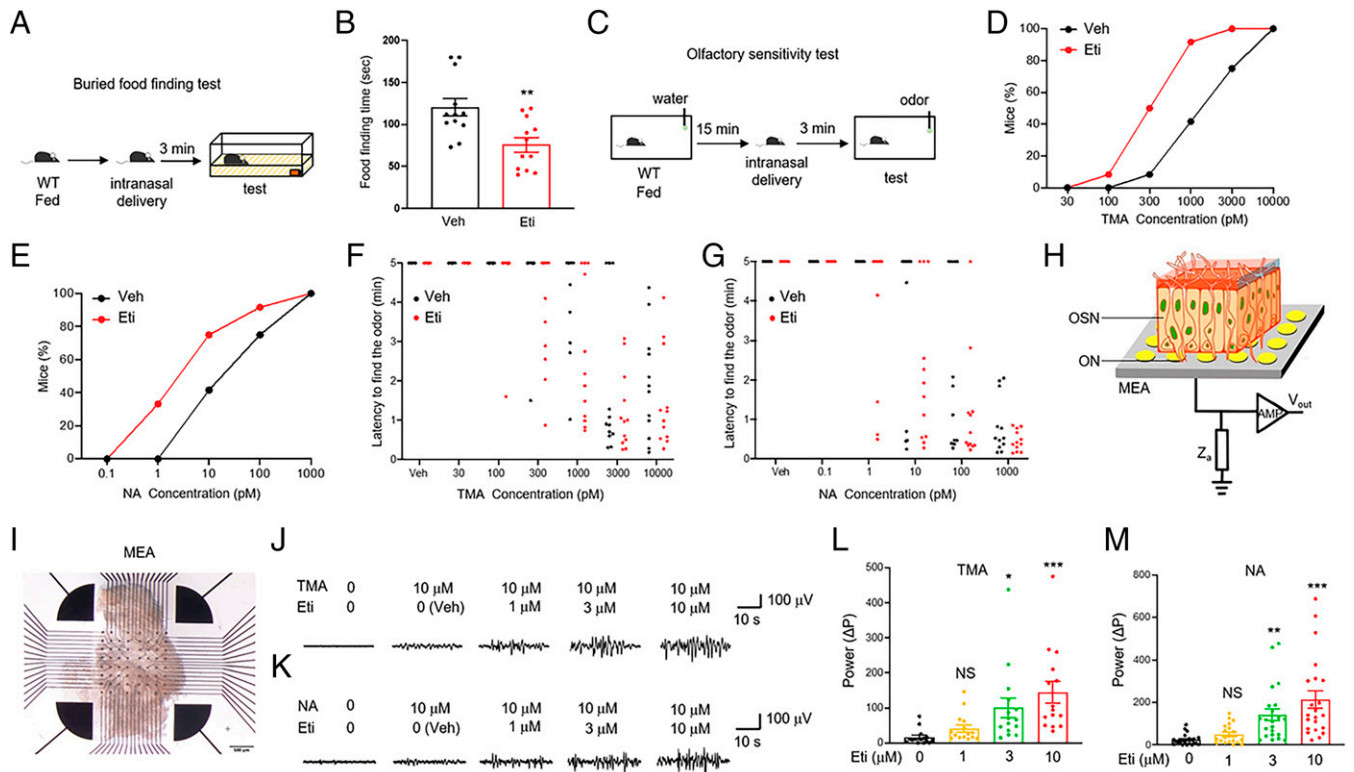
Fig. 3. Increase of olfactory function by acute inhibition of DRD2 in the mouse OM. (*A*) Experimental design. The WT fed mice that had normal access to food received intranasal delivery of vehicle (Veh) or DRD2 antagonist Eti, and 3 min later they were subjected to the buried food finding test. (*B*) Intranasal delivery of Eti (0.1 mg/kg) enhances olfactory abilities. The time to find the buried food was quantified. **$P = 0.0036$, two-sided t test, $n = 12$ mice per group. Data are presented as mean values ± SEM. (*C*) Experimental design. The WT fed mice were habituated in the testing cages for 15 min and then received intranasal treatment, and 3 min later the mice were subjected to the olfactory sensitivity test. (*D* and *E*) Olfactory sensitivity to TMA (*D*) and NA (*E*) was enhanced after intranasal treatment with Eti. Shown are the sniffing curves of mice treated with Veh or Eti. The *x* axis represents different concentrations of TMA or NA. The *y* axis indicates the percentage of the mice that found the odor source within 5 min. $n = 12$ mice per group. (*F* and *G*) Latency to find TMA (*F*) and NA (*G*) was shortened after intranasal application of Eti. Shown are the times taken to find the odor source TMA (*F*) and NA (*G*) in Veh- and Eti-treated mice. Each point depicts a single individual. Mice that failed to find the odorants in 5 min were plotted at 5. The *x* axis represents different concentrations of TMA or NA. The *y* axis indicates the latency to find the odor source. $P = 0.0024$ for TMA, $P = 0.0323$ for NA, the Scherier–Ray–Hare test, $n = 12$ mice per group. (*H*) Schematic diagram to show the OSN responses of OSN responses to odorants. ON, olfactory nerve; MEA, microelectrode array. (*I*) Diagram showing the OM tissues on the MEA during EOG recording. (*J* and *K*) DRD2 antagonist Eti increases OSN response to TMA (*J*) and NA (*K*) in a dose-dependent manner. Shown are the local field potential (LFP) of the mouse OM by ex vivo EOG recording. (*L*) Quantification of the relative power of LFP ($\Delta P = P_{Odor} - P_{Baseline}$) in *J*. NS, not significant ($P = 0.7432$), *$P = 0.0225$, ***$P = 0.0003$, compared with Veh, one-way ANOVA, $n = 15$ recording sites from four mice per group. Data are represented as mean values ± SEM. (*M*) Quantification of the relative power of LFP ($\Delta P = P_{Odor} - P_{Baseline}$) in *K*. NS, not significant ($P = 0.8167$), **$P = 0.0049$, ***$P < 0.0001$, compared with Veh, one-way ANOVA, $n = 21$ to 22 recording sites from four mice per group. Data are represented as mean values ± SEM.

Elevation of OSN Response to Odorants by Inhibition of DRD2 in the OM. The aforementioned data demonstrate that genetic deletion or intranasal inhibition of DRD2 can enhance olfactory sensitivity to TMA and NA. Next, we addressed whether inhibition of DRD2 in the OM could increase the OSN responses to TMA and NA. To avoid the influence from the central nervous system, we acutely isolated the tissues of OM and performed ex vivo electroolfactogram (EOG) recordings (Fig. 3 *H* and *I*). The OSN responses to odorants were quantified by the relative power (ΔP)—the power of local field potential after odorant stimulation subtracted from the power of local field potential at baselines. Both TMA and NA could induce a ΔP in mature OSNs, indicating a response of OSNs to odorants (Fig. 3 *J* and *K*). Strikingly, application of the DRD2 antagonist Eti in the recording solution for 3 min increased the ΔP of OSNs in a dose-dependent manner (Fig. 3 *L* and *M*). These results suggest that acute inhibition of DRD2 in the OM can enhance the OSN responses to odorants, which is in line with the behavioral findings that intranasal application of Eti increased the olfactory sensitivity (Fig. 2 *G–J*).

Attenuation of Olfactory Receptor Signaling by DA-DRD2. Since DRD2 is a $G_{\alpha i/o}$-coupled receptor (22) while most olfactory receptors are $G_{\alpha olf}/G_{\alpha s}$-linked receptors (46), we speculate

that the DA-DRD2 pathway can inhibit the cAMP signaling of olfactory receptors. The increase of cAMP caused by odorant binding to olfactory receptors leads to activation of protein kinase A (PKA) and phosphorylation of cAMP response element binding (CREB) protein, which promotes gene transcription (47) (Fig. 4*A*). To study whether DA-DRD2 can inhibit the cAMP signaling pathway of TAAR5 and MOR42-3, we performed a luciferase assay to analyze CREB-induced gene transcription downstream of olfactory receptors (48) in Hana3A cells transiently expressing DRD2 and TAAR5 or MOR42-3. The signaling curve of TAAR5 stimulated by different concentrations of TMA shifted rightward after DA treatment (Fig. 4*B*). These results suggest that DA-DRD2 can attenuate TMA-TAAR5 signaling (half-maximum effective concentration [EC$_{50}$] of TMA = 6.69 ± 1.48 μM with Veh, EC$_{50}$ of TMA = 21.06 ± 5.39 μM with 10 μM DA, $P < 0.0001$, two-way ANOVA, $n = 4$). The inhibitory effects of DA on TMA-TAAR5 signaling were specific because DA could not affect TMA-TAAR5 signaling in the absence of DRD2 (Fig. 4*C*). Moreover, DA-DRD2 inhibited TMA-TAAR5 signaling in a dose-dependent manner (IC$_{50}$ of DA = 0.022 ± 0.01 μM, $n = 4$) (Fig. 4*C*). Likewise, DA-DRD2 reduced NA-MOR42-3 signaling (EC$_{50}$ of NA = 29.35 ± 12.78 μM with vehicle [Veh], EC$_{50}$ of
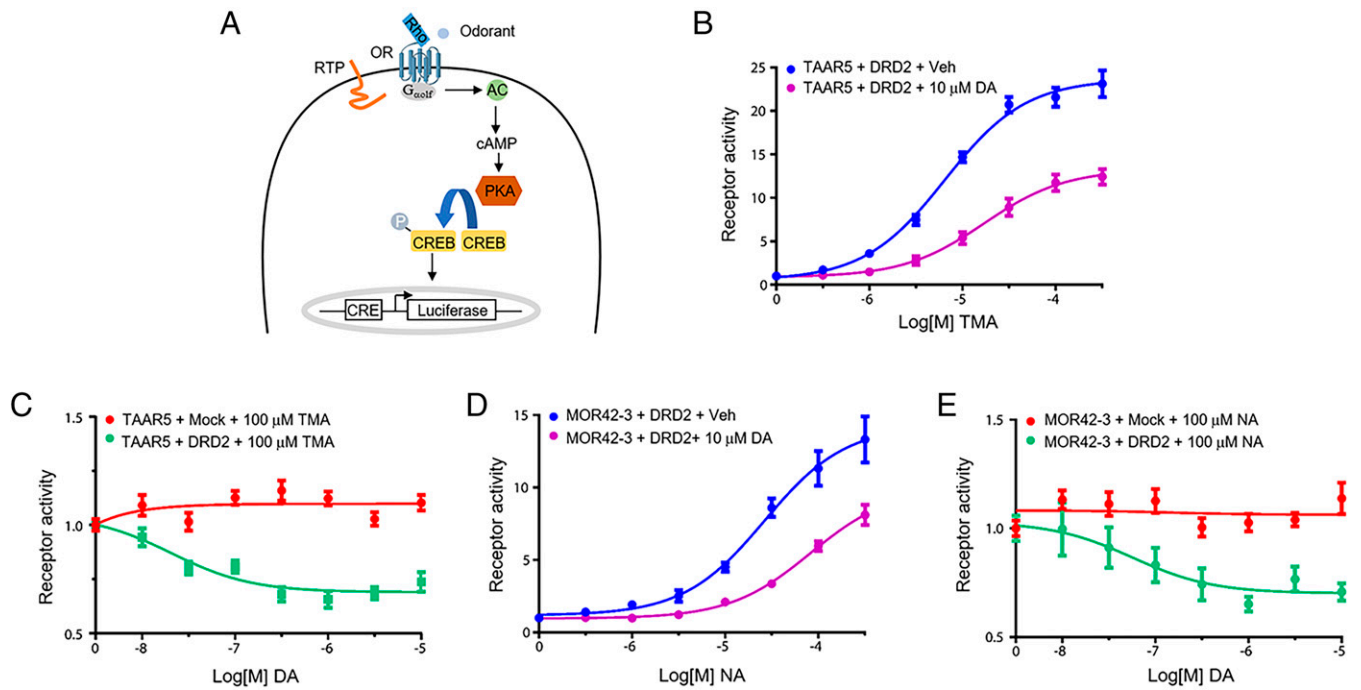
Fig. 4. DA-DRD2 inhibits cAMP signaling of TAAR5 and MOR42-3 in Hana3A cells. (*A*) Schematic diagram illustrating the principle of luciferase assay to study the cAMP signaling of olfactory receptors. Shown are the olfactory receptor signaling pathway in Hana3A cells. OR, olfactory receptor. RTP, receptor-transporting protein. PKA, protein kinase A; AC, adenylyl cyclase; CREB, cAMP response element binding protein; CRE, cAMP response element. (*B*) DA-DRD2 inhibited CRE-mediated transcription of TMA-TAAR5 signaling. Shown are the CRE luciferase curves of TMA-TAAR5 signaling. The *x* axis represents different concentrations of TMA scaled by $\log_{10}$. The *y* axis indicates the CRE luciferase activity. DRD2 and TAAR5 were cotransfected in Hana3A cells, and 18 h after transfection the cells were treated with different concentrations of TMA plus vehicle or 10 μM DA. The EC_{50} for TAAR5 in control cells is 6.69 ± 1.48 μM; The EC_{50} for TAAR5 in DA-treated cells is 21.06 ± 5.39 μM; $P < 0.0001$, two-way ANOVA, $n = 4$ independent experiments. Data are represented as mean values ± SEM. (*C*) DA inhibited CRE-mediated transcription of TMA-TAAR5 signaling in Hana3A cells coexpressing DRD2 and TAAR5 in a dose-dependent manner. Half-maximum inhibitory concentration (IC_{50}) of DA = 0.022 ± 0.01 μM, $n = 4$ independent experiments. Note that DA could not inhibit CRE-mediated transcription of TMA-TAAR5 signaling in the absence of DRD2. Data are represented as mean values ± SEM. (*D*) DA-DRD2 inhibited CRE-mediated transcription of NA-MOR42-3 signaling. Shown are the CRE luciferase curves of NA-MOR42-3 signaling. The *x* axis represents different concentrations of NA scaled by $\log_{10}$. The *y* axis indicates the CRE luciferase activity. DRD2 and MOR42-3 were cotransfected in Hana3A cells, and 18 h after transfection the cells were treated with different concentrations of NA plus vehicle or 10 μM DA. The EC_{50} for MOR42-3 in control cells is 29.35 ± 12.78 μM; the EC_{50} for MOR42-3 in DA-treated cells is 87.92 ± 17.31 μM; $P < 0.0001$, two-way ANOVA, $n = 4$ independent experiments. Data are represented as mean values ± SEM. (*E*) DA inhibited CRE-mediated transcription of NA-MOR42-3 signaling in Hana3A cells coexpressing DRD2 and MOR42-3 in a dose-dependent manner. $IC_{50} = 0.052 \pm 0.05$ μM, $n = 3$ independent experiments. Note that DA could not inhibit CRE-mediated transcription of NA-MOR42-3 signaling in the absence of DRD2. Data are represented as mean values ± SEM.

NA = 87.92 ± 17.31 μM with 10 μM DA, $P < 0.0001$, two-way ANOVA, $n = 4$) in a dose-dependent way (IC_{50} of DA = 0.052 ± 0.05 μM, $n = 3$) (Fig. 4 *D* and *E*). Collectively, these results demonstrate that DA-DRD2 can inhibit TMA- and NA-mediated olfactory receptor signaling.

Reduction of Local DA Synthesis in Mouse OM during Starvation. We next sought to address the physiological relevance of our finding that the DA-DRD2 pathway in mouse OM had a tonic inhibition on olfactory abilities. Starvation can enhance olfactory abilities across species, which is beneficial for food seeking and animal survival (4, 6). To determine whether DA levels in mouse OM change after starvation, we collected the OM from WT fed mice with normal access to food and WT fasted mice that were deprived of food for 24 h. The high-performance liquid chromatography (HPLC)-electrochemical detection results indicated that the concentration of DA, but not other monoamines such as 5-hydroxytryptamine (5-HT) or norepinephrine (NE), was significantly reduced in the OM from fasted mice, compared with fed mice (Fig. 5 *A–C* and *SI Appendix,* Fig. *S5A*). The reduction of DA in mouse OM during starvation could be due to decreased DA synthesis and/or increased DA degradation. However, both DA and its metabolite 3,4-dihydroxyphenylacetic acid (DOPAC) were reduced in the OM during starvation (Fig. 5 *A* and *B* and *SI Appendix,* Fig. *S5B*),

suggesting decrease of DA synthesis in the OM from fasted mice. By contrast, the concentrations of DA and 5-HT in the OB were similar between fed and fasted mice (*SI Appendix,* Fig. *S5C*). Altogether, these results indicate that DA synthesis was reduced in the OM during starvation in mice.

We further studied how starvation led to reduction of DA synthesis in mouse OM. The protein levels of TH, the rate-limiting enzyme for DA synthesis (19), were significantly down-regulated in the OM but not in the OB during starvation (Fig. 5 *D* and *E*). The TH proteins in the OM are from the sympathetic nerve terminals (17). In contrast, TH protein levels in the SCG where the somata of the sympathetic nerve was localized did not change in fasted mice (Fig. 5*F*). Altogether, these results suggest that starvation reduces the local TH protein levels in the sympathetic nerve terminals that innervate mouse OM.

The Th mRNA can be translated in the sympathetic nerve axons, which facilitates local DA synthesis (21, 49). To illustrate whether the reduced TH proteins in the OM from fasted mice results from a decrease of Th mRNA expression, we performed RT-qPCR on the mRNA extracts from mouse OM. Surprisingly, the Th mRNA levels were not significantly altered in the OM from fasted mice, compared to fed mice (Fig. 5 *G* and *H*). The ac[4]C modification of mRNA has recently been shown to promote translation efficiency in mammalian cells (50). To address whether starvation could affect the ac[4]C modification of Th
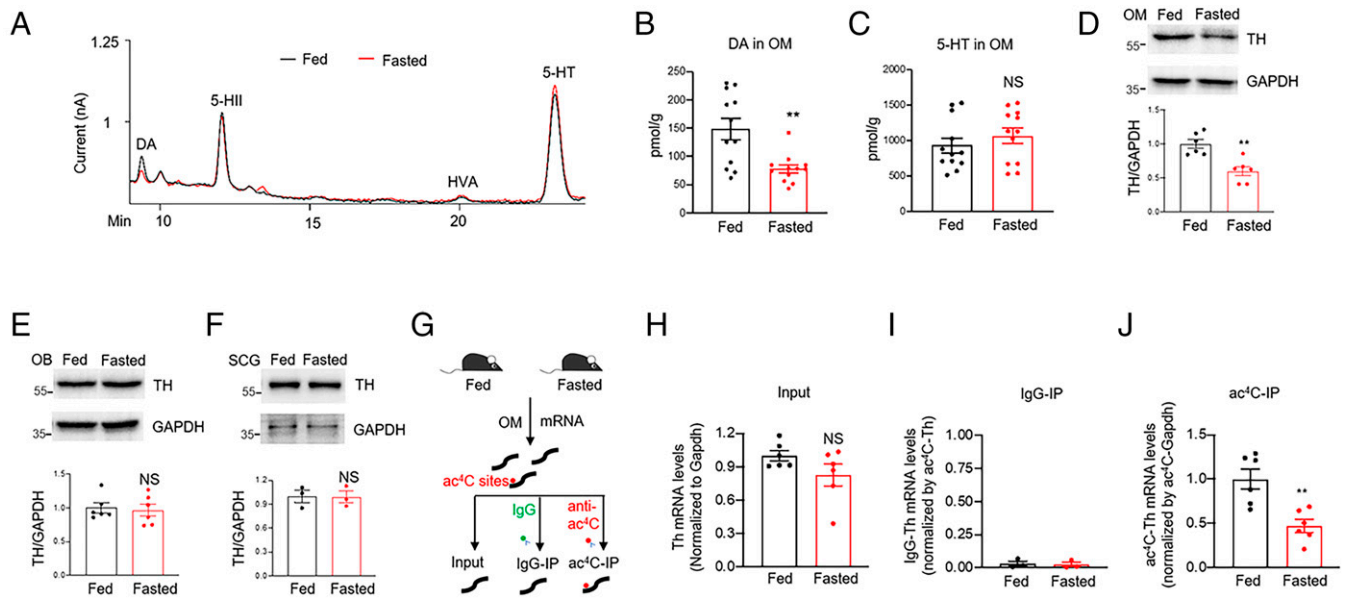
Fig. 5. Reduction of ac[4]C-Th mRNA and DA synthesis in mouse OM during starvation. (*A*) The HPLC curves of the monoamines in the homogenates of mouse OM. (*B*) DA levels were reduced in the OM from fasted mice, compared with fed mice. The concentrations of DA in mouse OM were quantified. **$P = 0.0018$, two-sided t test, $n = 12$ mice per group. Data were represented as mean values ± SEM. (*C*) The 5-HT levels were not altered in the OM from fasted mice, compared to fed mice. The concentrations of 5-HT in mouse OM were quantified. NS, not significant ($P = 0.3819$), two-sided t test, $n = 12$ mice per group. Data are represented as mean values ± SEM. (*D*) Reduction of TH protein levels in mouse OM during starvation. *Top*, representative blots. The homogenates of OM from fed and fasted mice were subjected to Western blot and probed with the indicated antibodies. *Bottom*, quantification of TH/GAPDH. The data were normalized to the fed group. **$P = 0.0019$, two-sided t test, $n = 6$ mice per group. Data are presented as mean values ± SEM. (*E*) No change of TH protein levels in mouse OB during starvation. *Top*, representative blots. The homogenates of OB from fed and fasted mice were subjected to Western blot and probed with the indicated antibodies. *Bottom*, quantification of TH/GAPDH. The data were normalized to the fed group. NS, not significant $P = 0.7831$, two-sided t test, $n = 6$ mice per group. Data are presented as mean values ± SEM. (*F*) No change of TH protein levels in mouse SCG during starvation. *Top*, representative blots. The homogenates of SCG from fed and fasted mice were subjected to Western blot and probed with the indicated antibodies. *Bottom*, quantification of TH/GAPDH. The data were normalized to the control group. NS, not significant ($P = 0.9301$), two-sided t test, $n = 3$ mice per group. Data are presented as mean values ± SEM. (*G*) Experimental design. The mRNA purified from the OM in fed and fasted mice were immunoprecipitated by IgG or anti-ac[4]C antibodies. The mRNA from the total lysates (input) or immunoprecipitation was subjected to RT-qPCR. (*H*) Total Th mRNA levels were not altered in the OM from fasted mice, compared to fed mice. The Th mRNA levels were normalized to that of Gapdh. NS, not significant ($P = 0.1396$), two-sided t test, $n = 6$ mice per group. Data are presented as mean values ± SEM. (*I*) Th mRNA was not detectable in the immunoprecipitation with IgG, compared with anti-ac[4]C antibodies. (*J*) ac[4]C-Th mRNA levels were reduced in the OM from fasted mice, compared to fed mice. The ac[4]C-TH mRNA levels were normalized by that of ac[4]C-Gapdh mRNA. **$P = 0.003$, two-sided t test, $n = 6$ independent experiments. Data are presented as mean values ± SEM.

mRNA in mouse OM, we performed acetylated RNA immunoprecipitation (acRIP) followed by RT-qPCR to quantitively compare the acetylated Th mRNA levels (Fig. 5*G*). The mRNA levels were very low when immunoprecipitated with IgG, compared with anti-ac[4]C antibodies (Fig. 5*I*), indicating the specificity of acRIP. The results showed that the ac[4]C-Th mRNA levels were significantly decreased in the OM from fasted mice, compared with fed mice (Fig. 5*J*). Altogether, these results suggest that starvation down-regulates the ac[4]C modification of Th mRNA and thus reduces local TH proteins and DA synthesis in mouse OM.

Requirement of Nasal DA Reduction in Starvation-Induced Olfactory Enhancement. Next, we investigated whether DA reduction in the OM was required for the enhanced olfactory abilities in fasted mice. Toward this goal, we treated the WT fasted mice with DA (8 μM in 10 μL saline) or vehicle through intranasal delivery 3 min before the buried food finding test (Fig. 6*A*). The DA concentration in the fasted mouse OM 3 min after intranasal delivery of DA reached 136.4 pmol/g (Fig. 6*B*), which is similar to the DA levels in the OM of fed mice (Fig. 5*B*). Strikingly, intranasal application of DA significantly increased the time taken to find the buried food in fasted mice, compared with vehicle-treated fasted mice (Fig. 6*C*). Furthermore, the time taken to find the buried food in DA-treated fasted mice was comparable to that in fed mice (Fig. 6*C*), suggesting that the DA pathway is the key player in olfactory regulation during starvation. By contrast,

intranasal treatment with DA did not change the locomotion or the time to find the visible food in WT fasted mice (*SI Appendix,* Fig. S6), excluding other nonolfactory effects. These results demonstrate that intranasal delivery of DA can reverse the enhanced olfactory abilities in WT fasted mice, supporting a necessary role of nasal DA reduction in the starvation-induced olfactory enhancement.

Although intranasal delivery of DA increased the time taken to find the buried food in fasted Omp[Cre/+] mice, DA had no effects on food finding in fasted Omp-Drd2^{−/−} mice (Fig. 6*D*). This result indicates that intranasal treatment with DA attenuates olfactory abilities through DRD2 expressed in mature OSNs in fasted mice. Note that the vehicle-treated Omp-Drd2^{−/−} mice performed better in the buried food finding tests, compared with vehicle-treated controls during starvation (Fig. 6*D*), which supports the previous finding that DRD2 in the mature OSNs has a tonic inhibition on olfaction (Fig. 2). Altogether, these results suggest that intranasal application of DA can reduce the olfactory abilities through DRD2 in mature OSNs in fasted mice.

Attenuation of Olfaction during Starvation by Acute Activation of Nasal DRD2. To investigate whether acute activation of nasal DRD2 could attenuate olfaction during starvation, we treated fasted mice with sumanirole maleate (Sum, 0.1 mg/kg) (51), a DRD2 agonist or vehicle via intranasal delivery 3 min before the buried food finding test. Intranasal application of Sum
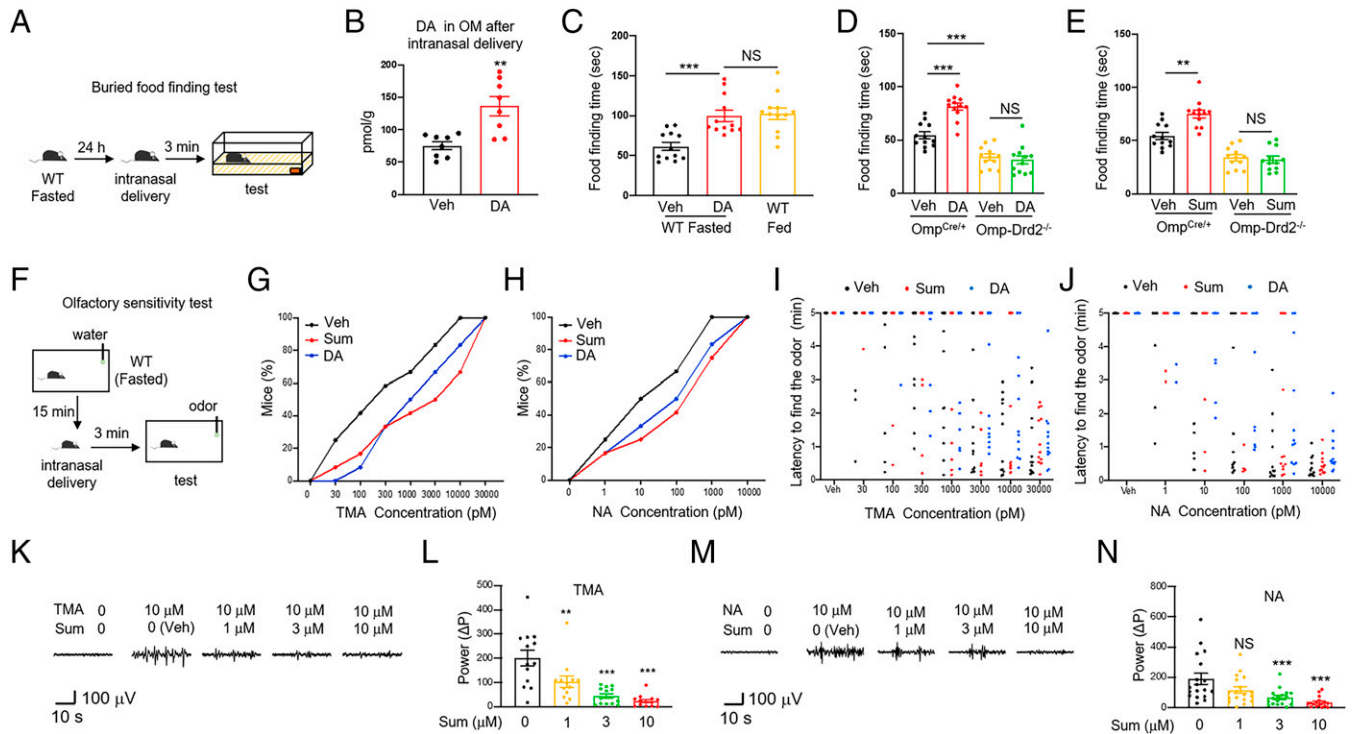
Fig. 6. A necessary role of nasal DA reduction in starvation-induced olfactory enhancement. (*A*) Experimental design. The WT fasted mice that were deprived of food for 24 h received intranasal delivery of Veh or reagents, and 3 min later they were subjected to the buried food finding test. (*B*) DA levels were increased in the OM 3 min after intranasal delivery of DA, compared with vehicle. The concentrations of DA in mouse OM were quantified. **$P = 0.0018$, two-sided t test, $n = 8$ mice per group. Data were represented as mean values ± SEM. (*C*) Intranasal delivery of DA (8 μM in 10 μL saline) in fasted mice attenuates the olfactory abilities to the levels of fed mice. The time to find the buried food in different groups of mice was quantified. NS, not significant ($P = 0.955$), ***$P = 0.0006$, one-way ANOVA, $n = 12$ mice per group. Data are presented as mean values ± SEM. (*D*) Intranasal delivery of DA (8 μM in 10 μL saline) inhibited the olfactory abilities through DRD2 in mature OSNs. Note that DA attenuates olfaction in control mice but not in Omp-Drd2$^{-/-}$ mice. The time to find the buried food in different groups of mice was quantified. NS, not significant ($P = 0.9757$), ***$P < 0.0001$, Omp$^{Cre/+}$ + Veh vs. Omp$^{Cre/+}$ + DA, ***$P = 0.0009$, Omp$^{Cre/+}$ + Veh vs. Omp-Drd2$^{-/-}$ + Veh, two-way ANOVA followed by Sidak's multiple comparisons test, $n = 12$ mice per group. Data are presented as mean values ± SEM. (*E*) Intranasal delivery of DRD2 agonist Sum (0.1 mg/kg) inhibited the olfactory abilities in fasted mice through DRD2 in mature OSNs. Note that Sum attenuates olfaction in control mice but not in Omp-Drd2$^{-/-}$ mice. The time to find the buried food in different groups of mice was quantified. NS, not significant ($P = 0.9996$), **$P = 0.0081$, two-way ANOVA followed by Sidak's multiple comparisons test, $n = 12$ mice per group. Data are presented as mean values ± SEM. (*F*) Experimental design. The WT fasted mice were habituated in the testing cages for 15 min and then they received intranasal treatment, and 3 min later the mice were subjected to the olfactory sensitivity test. (*G* and *H*) Olfactory sensitivity to TMA (*G*) and NA (*H*) was attenuated after intranasal treatment with DA (8 μM in 10 μL saline) and Sum (0.1 mg/kg) in WT fasted mice. Shown are the sniffing curves of mice treated with Veh, DA, or Sum. The x axis represents different concentrations of TMA or NA. The y axis indicates the percentage of the mice that found the odor source within 5 min. $n = 12$ mice per group. (*I* and *J*) Latency to find TMA (*I*) and NA (*J*) was increased after intranasal application of DA and Sum in WT fasted mice. Shown are the times taken to find the odor source TMA (*I*) and NA (*J*) in Veh-, DA-, and Sum-treated mice. Each point depicts a single individual. Mice that failed to find the odorants in 5 min were plotted at 5. The x axis represents different concentrations of TMA or NA. The y axis indicates the latency to find the odor source. Veh vs. Sum, $P = 0.038$ for TMA, $P = 0.0288$ for NA; Veh vs. DA, $P = 0.0049$ for TMA, $P = 0.0018$ for NA, the Scherier–Ray–Hare test, $n = 12$ mice per group. (*K*) The DRD2 agonist Sum attenuated OSN response to TMA from WT fasted mice in a dose-dependent manner. Shown are the local field potential (LFP) of the mouse OM by ex vivo EOG recordings. (*L*) Quantification of the relative power of LFP ($\Delta P = P_{Odor} - P_{Baseline}$) in *K*. **$P = 0.0045$, ***$P < 0.0001$, compared with Veh, one-way ANOVA, $n = 13$ recording sites from four mice per group. Data are presented as mean values ± SEM. (*M*) The DRD2 agonist Sum dose-dependently attenuates OSN response to NA from WT fasted mice. Shown are the LFP of the OM tissues through ex vivo EOG recordings. (*N*) Quantification of the relative power of LFP ($\Delta P = P_{Odor} - P_{Baseline}$) in *M*. NS, not significant ($P = 0.0625$), ***$P = 0.0009$ for 3 μM Sum, ***$P < 0.0001$ for 10 μM Sum, compared with Veh, one-way ANOVA, $n = 17$ to 18 recording sites from four mice per group. Data are presented as mean values ± SEM.

significantly increased the time taken to find the buried food in fasted Omp$^{Cre/+}$ mice, but not in the fasted Omp-Drd2$^{-/-}$ mice (Fig. 6*E*). Intranasal treatment with Sum did not alter the locomotion or the time taken to find the visible food in WT fasted mice (*SI Appendix*, Fig. S6), excluding other nonolfactory effects. These data indicate that intranasal delivery with Sum attenuates olfaction mainly through DRD2 in mature OSNs during starvation.

To further study whether acute activation of DRD2 in the nose could reduce the olfactory sensitivity in WT fasted mice, we performed intranasal delivery of DA, Sum, or vehicle 3 min before the olfactory sensitivity test (Fig. 6*F*). Again, we analyzed the olfactory sensitivity to TMA and NA. As shown in Fig. 6 *G* and *H*, the sniffing curves toward different concentrations of TMA and NA shifted rightward in DA- and Sum-treated mice, compared with vehicle-treated mice. A total of 58.3% (7/12) of

control mice could find 300 pM TMA in 5 min, whereas only 33.3% (4/12) of DA-treated mice and 33.3% (4/12) of Sum-treated mice could (Fig. 6*G*). A total of 50% (6/12) of control mice could find 10 pM NA in 5 min, whereas only 33.3% (4/12) of DA-treated mice and 25% (3/12) of Sum-treated mice could (Fig. 6*H*). Likewise, the latency to find the odor source of TMA and NA is significantly increased in DA- and Sum-treated mice, compared with vehicle-treated mice (Fig. 6 *I* and *J*). All these results demonstrate that intranasal activation of DRD2 can attenuate olfactory sensitivity in WT fasted mice.

Next, we explored whether acute activation of nasal DRD2 from WT fasted mice could reduce OSN responses to TMA and NA. Toward this goal, we acutely isolated the OM from WT fasted mice and performed ex vivo EOG recordings. The OSN responses to odorants were quantified by the relative power (ΔP)—the power of local field potential after odorant
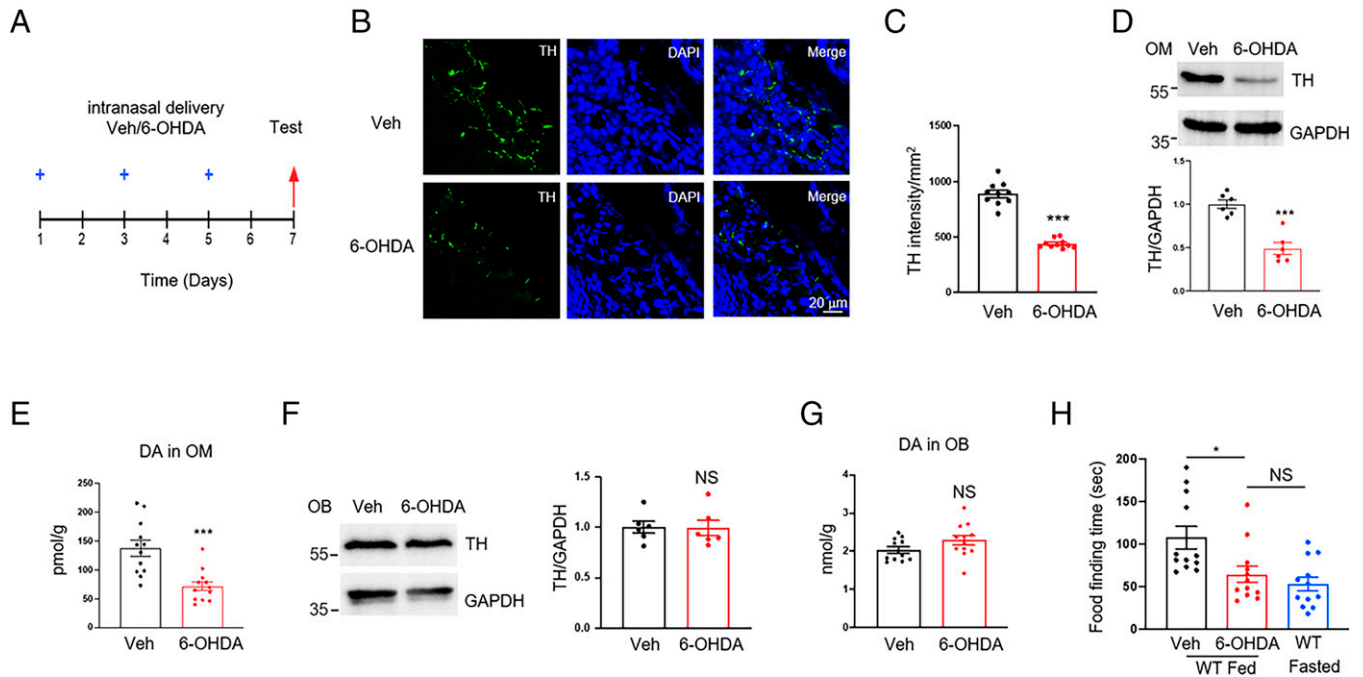
Fig. 7. Olfactory enhancement after down-regulation of DA in mouse OM. (*A*) Experimental design. WT fed mice received intranasal treatment of 6-OHDA (100 mg/kg) or Veh (saline containing 0.1% ascorbic acid) every other day for 6 d and then were subjected to immunostaining, Western blot, and buried food finding tests on day 7. (*B*) Destruction of sympathetic nerve terminals after intranasal application of 6-OHDA for 6 d. The OM slices from vehicle and 6-OHDA–treated mice were stained with anti-TH, a marker for sympathetic nerve terminals. (Scale bar, 20 μm.) (*C*) Quantification of the TH immunofluorescent intensity in *B*. ***$P < 0.0001$, two-sided t test, $n = 10$ slices from three mice per group. Data are presented as mean values ± SEM. (*D*) Reduction of TH protein levels in mouse OM after intranasal application of 6-OHDA for 6 d. *Top*, representative blots. The homogenates of OM from vehicle and 6-OHDA–treated mice were subjected to Western blot and probed with the indicated antibodies. *Bottom*, quantification of TH/GAPDH. The data were normalized to the control group. ***$P = 0.0001$, two-sided t test, $n = 6$ mice per group. Data are presented as mean values ± SEM. (*E*) Decrease of DA levels in mouse OM after intranasal application of 6-OHDA for 6 d. The homogenates of OM tissues from vehicle and 6-OHDA–treated mice were subjected to HPLC-electrochemical detection assay to determine the DA concentration. ***$P = 0.0004$, two-sided t test, $n = 12$ mice per group. Data are presented as mean values ± SEM. (*F*) No changes of TH protein levels in mouse OB after intranasal application of 6-OHDA for 6 d. *Left*, representative blots. The homogenates of OB from vehicle and 6-OHDA–treated mice were subjected to Western blot and probed with the indicated antibodies. *Right*, quantification of TH/GAPDH. The data were normalized to the control group. NS, not significant ($P = 0.9471$), two-sided t test, $n = 6$ mice per group. Data are presented as mean values ± SEM. (*G*) No alteration of DA levels in mouse OB after intranasal application of 6-OHDA for 6 d. The homogenates of OB from vehicle and 6-OHDA–treated mice were subjected to HPLC-electrochemical detection assay to determine the DA concentration. NS, not significant ($P = 0.1112$), two-sided t test, $n = 12$ mice per group. Data are presented as mean values ± SEM. (*H*) Intranasal delivery of 6-OHDA in WT fed mice increased the olfactory abilities to the levels of WT fasted mice. The time to find the buried food in different groups of mice was quantified. NS, not significant ($P = 0.7231$), *$P = 0.0176$, one-way ANOVA, $n = 12$ mice per group. Data are presented as mean values ± SEM.

stimulation subtracted from the power of local field potential at baselines. Application of the DRD2 agonist Sum in the recording solution decreased the ΔP of OSNs in a dose-dependent manner (Fig. 6 *K–N*). These results suggest that acute activation of DRD2 in the OM from WT fasted mice can reduce OSN responses to odorants.

Enhanced Olfaction by Down-Regulation of DA Synthesis in Mouse OM. We reasoned that if DA reduction in mouse OM is important for the olfactory enhancement during starvation, down-regulation of DA in the OM from WT fed mice should mimic the enhanced olfaction in fasted mice. To test this hypothesis, we performed intranasal delivery of 6-hydroxy-dopamine (6-OHDA, 100 mg/kg) (52) or vehicle in WT fed mice every other day, and the olfactory behaviors were tested 2 d after three treatments (Fig. 7*A*). In the mouse OM, the sympathetic nerve endings revealed by the immunofluorescence of TH were mainly distributed in the layer of lamina propria (LP) just beneath the layer of olfactory epithelium (*SI Appendix*, Fig. S7*A*). 6-OHDA is commonly used to destruct the sympathetic nerve terminals (53). After intranasal treatment of 6-OHDA, the number of sympathetic nerve endings indicated by the immunostaining of TH was greatly reduced in the LP (Fig. 7 *B* and *C*). In agreement, intranasal delivery of 6-OHDA led to a significant decrease of TH proteins in the OM (Fig. 7*D*). Since TH is the rate-limiting enzyme for DA synthesis (19), the

DA levels were greatly down-regulated in the OM after intranasal treatment with 6-OHDA (Fig. 7*E*). By contrast, neither the TH proteins nor the DA concentration were altered in the OB after intranasal application of 6-OHDA (Fig. 7 *F* and *G*). These results indicate that intranasal delivery of 6-OHDA specifically reduced DA levels in the OM but not in the OB.

We next performed the buried food finding test after 6-OHDA treatment. As shown in Fig. 7*H*, the time to find the buried food was significantly reduced in WT fed mice treated with 6-OHDA, compared with WT fed mice treated with vehicle. Of note, the time to find the buried food in WT fed mice after 6-OHDA treatment was similar to that in WT fasted mice (Fig. 7*H*). By contrast, intranasal application of 6-OHDA did not alter the locomotion or the time to find the visible food in WT fed mice (*SI Appendix*, Fig. S7 *B–F*), excluding other nonolfactory effects. Altogether, these results demonstrate that reduction of DA in mouse OM is sufficient to increase olfactory abilities.

Discussion

Our results demonstrate that nasal DA and DRD2 receptor may serve as the peripheral targets for olfactory modulation in mice. Intranasal delivery of 6-OHDA that destructs the sympathetic nerve terminals (53) leads to reduction of DA in the OM, which supports the hypothesis that the major source of DA in the OM is from sympathetic nerves (17). The activities

of sympathetic nerves are decreased during starvation (54), which is consistent with reduction of DA synthesis in the nerve terminals in the OM from hungry mice. We also provide ex vivo and in vivo evidence that DA-DRD2 signaling in the mature OSNs has a tonic inhibition on odor response.

The findings presented here might have a potential application to humans. Firstly, the TH-positive nerve terminals are also distributed in human OM (55, 56), which suggests that DA can be produced locally in the human nose. Secondly, DRD2 is also expressed in the mature OSNs from human (39). Lastly, DA overflow is observed in schizophrenia patients, and DRD2 is the target of several antipsychotic drugs (23, 24). Our finding that intranasal application of DRD2 antagonist Eti could increase olfactory abilities might be beneficial for the treatment of olfactory dysfunction in patients with psychiatric disorders. It should be noted that Eti might have effects on olfaction beyond the nose. Because the food finding time is already significantly reduced in OMP-Drd2$^{-/-}$ mice compared with WT mice, testing Eti effects in the nose of OMP-Drd2$^{-/-}$ mice does not rule out redundant effects of Eti in the brain or elsewhere.

We also show that DRD2 is expressed in the cilia of mature OSNs. In addition, the luciferase assay indicates that DA-DRD2 attenuates odor-induced cAMP signaling of TAAR5 and MOR24-3. We also provide evidence that DRD2 is coexpressed with TAAR5 or MOR24-3 in the mature OSNs. Based on these facts, it is possible that DA-DRD2 directly inhibits ciliary cAMP signaling of olfactory receptors and thus reduces odor responses. Given that DRD2 is also expressed in the somata of mature OSNs, DA-DRD2 could also inhibit cAMP signaling in the somata and in turn affect voltage gated ion channels and cell excitability (57, 58). Regardless, our results demonstrate potential mechanisms underlying the peripheral regulation of olfaction.

Unlike the olfactory receptor genes, which follow the principle of "one receptor, one neuron" (59), a large population of mature OSNs express Drd2, which is conserved among humans, rats, and mice (35, 39, 60). Future studies are warranted to investigate whether DA-DRD2 can inhibit the odor signaling of other olfactory receptors in addition to TAAR5 and MOR24-3. In sum, our results reveal nasal DA and DRD2 receptor as the potential peripheral targets for olfactory modulation, which may open the door to new approaches for olfactory regulation in both health and disease.

Materials and Methods

Further information and request for resources should be made to D.-M.Y. at dmyin@brain.ecnu.edu.cn. Raw data of Western blot is presented in *SI Appendix*, Fig. S8.

Treatment and Analysis of the Mice. Male mice aged at 2.5 to 3 mo were used in all experiments. The detailed information of transgenic mouse lines is available in *SI Appendix*. The OM tissues and slices were prepared and analyzed by histological, biochemical, and EOG methods as indicated in *SI Appendix*. The mice were treated with DRD2 agonist and antagonist through intranasal delivery, and the olfactory behavioral tests were performed as indicated in *SI Appendix*.

Cell Culture Experiments. Hana3A cells were used for the luciferase assay of olfactory receptor signaling as indicated in *SI Appendix*.

Data Availability. All data are included in the article and *SI Appendix*.

Author affiliations: [a]Key Laboratory of Brain Functional Genomics, Ministry of Education and Shanghai, School of Life Science, East China Normal University, Shanghai 200062, China; [b]Biosensor National Special Laboratory, Key Laboratory for Biomedical Engineering of Education Ministry, Department of Biomedical Engineering, Zhejiang University, Hangzhou 310027, China; [c]Center for Brain Science, Shanghai Children's Medical Center, School of Medicine, Shanghai Jiao Tong University, Shanghai 200127, China; [d]Department of Anatomy and Physiology, Ministry of Education-Shanghai Key Laboratory of Children's Environmental Health in Xinhua Hospital, Shanghai Jiao Tong University School of Medicine, Shanghai 200025, China; and [e]Shanghai Research Center for Brain Science and Brain-Inspired Intelligence, Shanghai 201210, China

1. K. L. Whitcroft, T. Hummel, Olfactory dysfunction in COVID-19: Diagnosis and management. *JAMA* **323**, 2512–2514 (2020).
2. P. J. Moberg *et al.*, Olfactory dysfunction in schizophrenia: A qualitative and quantitative review. *Neuropsychopharmacology* **21**, 325–340 (1999).
3. R. I. Mesholam, P. J. Moberg, R. N. Mahr, R. L. Doty, Olfaction in neurodegenerative disease: A meta-analysis of olfactory functioning in Alzheimer's and Parkinson's diseases. *Arch. Neurol.* **55**, 84–90 (1998).
4. P. Sengupta, The belly rules the nose: Feeding state-dependent modulation of peripheral chemosensory responses. *Curr. Opin. Neurobiol.* **23**, 68–75 (2013).
5. Q. Li, S. D. Liberles, Aversion and attraction through olfaction. *Curr. Biol.* **25**, R120–R129 (2015).
6. B. Palouzier-Paulignan *et al.*, Olfaction under metabolic influences. *Chem. Senses* **37**, 769–797 (2012).
7. C. M. Root, K. I. Ko, A. Jafari, J. W. Wang, Presynaptic facilitation by neuropeptide signaling mediates odor-driven food search. *Cell* **145**, 133–144 (2011).
8. M. L. Andermann, B. B. Lowell, Toward a wiring diagram understanding of appetite control. *Neuron* **95**, 757–778 (2017).
9. S. Rengarajan, K. A. Yankura, M. L. Guillermin, W. Fung, E. A. Hallem, Feeding state sculpts a circuit for sensory valence in *Caenorhabditis elegans*. *Proc. Natl. Acad. Sci. U.S.A.* **116**, 1776–1781 (2019).
10. K. Vogt *et al.*, Internal state configures olfactory behavior and early sensory processing in *Drosophila* larvae. *Sci. Adv.* **7**, eabd6900 (2021).
11. N. Horio, S. D. Liberles, Hunger enhances food-odour attraction through a neuropeptide Y spotlight. *Nature* **592**, 262–266 (2021).
12. M. T. Lucero, Peripheral modulation of smell: Fact or fiction? *Semin. Cell Dev. Biol.* **24**, 58–70 (2013).
13. A. Carlsson, M. Lindqvist, T. Magnusson, 3,4-Dihydroxyphenylalanine and 5-hydroxytryptophan as reserpine antagonists. *Nature* **180**, 1200 (1957).
14. A. Carlsson, M. Lindqvist, T. Magnusson, B. Waldeck, On the presence of 3-hydroxytyramine in brain. *Science* **127**, 471 (1958).
15. C. Bell, Dopamine release from sympathetic nerve terminals. *Prog. Neurobiol.* **30**, 193–208 (1988).
16. M. O. Thorner, Dopamine is an important neurotransmitter in the autonomic nervous system. *Lancet* **1**, 662–665 (1975).
17. T. Kawano, F. L. Margolis, Catecholamines in olfactory mucosa decline following superior cervical ganglionectomy. *Chem. Senses* **10**, 353–356 (1985).
18. F. Mignini, D. Tomassoni, E. Traini, F. Amenta, Dopamine, vesicular transporters and dopamine receptor expression and localization in rat thymus and spleen. *J. Neuroimmunol.* **206**, 5–13 (2009).
19. T. Nagatsu, Tyrosine hydroxylase: Human isoforms, structure and regulation in physiology and pathology. *Essays Biochem.* **30**, 15–35 (1995).
20. H. Thoenen, R. A. Mueller, J. Axelrod, Phase difference in the induction of tyrosine hydroxylase in cell body and nerve terminals of sympathetic neurones. *Proc. Natl. Acad. Sci. U.S.A.* **65**, 58–62 (1970).
21. N. M. Gervasi *et al.*, The local expression and trafficking of tyrosine hydroxylase mRNA in the axons of sympathetic neurons. *RNA* **22**, 883–895 (2016).
22. J. A. Gingrich, M. G. Caron, Recent advances in the molecular biology of dopamine receptors. *Annu. Rev. Neurosci.* **16**, 299–321 (1993).
23. S. H. Snyder, The dopamine hypothesis of schizophrenia: Focus on the dopamine receptor. *Am. J. Psychiatry* **133**, 197–202 (1976).
24. D. F. Wong *et al.*, Positron emission tomography reveals elevated D2 dopamine receptors in drug-naive schizophrenics. *Science* **234**, 1558–1563 (1986).
25. T. Arinami *et al.*, Association of dopamine D2 receptor molecular variant with schizophrenia. *Lancet* **343**, 703–704 (1994).
26. K. Blum *et al.*, Allelic association of human dopamine D2 receptor gene in alcoholism. *JAMA* **263**, 2055–2060 (1990).

27. S. Wang et al.; Tourette International Collaborative Genetics Study (TIC Genetics); Tourette Syndrome Genetics Southern and Eastern Europe Initiative (TSGENESEE); Tourette Association of America International Consortium for Genetics (TAAICG), De novo sequence and copy number variants are strongly associated with tourette disorder and implicate cell polarity in pathogenesis. *Cell Rep.* **24**, 3441–3454.e12 (2018).

28. B. V. Halldorsson et al., Characterizing mutagenic effects of recombination through a sequence-level genetic map. *Science* **363**, eaau1043 (2019).

29. A. Usiello et al., Distinct functions of the two isoforms of dopamine D2 receptors. *Nature* **408**, 199–203 (2000).

30. T. X. Xu et al., Hyperdopaminergic tone erodes prefrontal long-term potential via a D2 receptor-operated protein phosphatase gate. *J. Neurosci.* **29**, 14086–14099 (2009).

31. A. Y. Hsia, J. D. Vincent, P. M. Lledo, Dopamine depresses synaptic inputs into the olfactory bulb. *J. Neurophysiol.* **82**, 1082–1085 (1999).

32. M. Ennis et al., Dopamine D2 receptor-mediated presynaptic inhibition of olfactory nerve terminals. *J. Neurophysiol.* **86**, 2986–2997 (2001).

33. Y. Q. Zhang et al., Dopamine D2 receptor regulates cortical synaptic pruning in rodents. *Nat. Commun.* **12**, 6444 (2021).

34. L. Tan, Q. Li, X. S. Xie, Olfactory sensory neurons transiently express multiple olfactory receptors during development. *Mol. Syst. Biol.* **11**, 844 (2015).

35. Q. Yu et al., Genetic labeling reveals temporal and spatial expression pattern of D2 dopamine receptor in rat forebrain. *Brain Struct. Funct.* **224**, 1035–1049 (2019).

36. V. Coronas, L. K. Srivastava, J. J. Liang, F. Jourdan, E. Moyse, Identification and localization of dopamine receptor subtypes in rat olfactory mucosa and bulb: A combined in situ hybridization and ligand binding radioautographic approach. *J. Chem. Neuroanat.* **12**, 243–257 (1997).

37. H. Yamaguchi et al., Dopamine D2 receptor plays a critical role in cell proliferation and proopiomelanocortin expression in the pituitary. *Genes Cells* **1**, 253–268 (1996).

38. T. Stojanovic et al., Validation of dopamine receptor DRD1 and DRD2 antibodies using receptor deficient mice. *Amino Acids* **49**, 1101–1109 (2017).

39. M. A. Durante et al., Single-cell analysis of olfactory neurogenesis and differentiation in adult humans. *Nat. Neurosci.* **23**, 323–326 (2020).

40. J. Li, T. Ishii, P. Feinstein, P. Mombaerts, Odorant receptor gene choice is reset by nuclear transfer from mouse olfactory sensory neurons. *Nature* **428**, 393–399 (2004).

41. E. P. Bello et al., Cocaine supersensitivity and enhanced motivation for reward in mice lacking dopamine D2 autoreceptors. *Nat. Neurosci.* **14**, 1033–1038 (2011).

42. M. Yang, J. N. Crawley, Simple behavioral assessment of mouse olfaction. *Curr. Protoc. Neurosci.* **Chapter 8**, Unit 8 24 (2009).

43. S. D. Liberles, L. B. Buck, A second class of chemosensory receptors in the olfactory epithelium. *Nature* **442**, 645–650 (2006).

44. T. Abaffy, A. Malhotra, C. W. Luetje, The molecular basis for ligand specificity in a mouse olfactory receptor: A network of functionally important residues. *J. Biol. Chem.* **282**, 1216–1224 (2007).

45. P. Svenningsson et al., Regulation of the phosphorylation of the dopamine- and cAMP-regulated phosphoprotein of 32 kDa in vivo by dopamine D1, dopamine D2, and adenosine A2A receptors. *Proc. Natl. Acad. Sci. U.S.A.* **97**, 1856–1860 (2000).

46. L. Buck, R. Axel, A novel multigene family may encode odorant receptors: A molecular basis for odor recognition. *Cell* **65**, 175–187 (1991).

47. G. A. Gonzalez, M. R. Montminy, Cyclic AMP stimulates somatostatin gene transcription by phosphorylation of CREB at serine 133. *Cell* **59**, 675–680 (1989).

48. H. Zhuang, H. Matsunami, Evaluating cell-surface expression and measuring activation of mammalian odorant receptors in heterologous cells. *Nat. Protoc.* **3**, 1402–1413 (2008).

49. A. Aschrafi, A. E. Gioio, L. Dong, B. B. Kaplan, Disruption of the axonal trafficking of tyrosine hydroxylase mRNA impairs catecholamine biosynthesis in the axons of sympathetic neurons. *eNeuro* **4**, ENEURO.0385-16.2017 (2017).

50. D. Arango et al., Acetylation of cytidine in mRNA promotes translation efficiency. *Cell* **175**, 1872–1886.e1824 (2018).

51. G. T. Collins, J. A. Jackson, W. Koek, C. P. France, Effects of dopamine D(2)-like receptor agonists in mice trained to discriminate cocaine from saline: Influence of feeding condition. *Eur. J. Pharmacol.* **729**, 123–131 (2014).

52. A. Kondo, A. Togari, In vivo stimulation of sympathetic nervous system modulates osteoblastic activity in mouse calvaria. *Am. J. Physiol. Endocrinol. Metab.* **285**, E661–E667 (2003).

53. G. Cohen et al., Destruction of sympathetic nerve terminals by 6-hydroxydopamine: Protection by 1-phenyl-3-(2-thiazolyl)-2-thiourea, diethyldithiocarbamate, methimazole, cysteamine, ethanol and n-butanol. *J. Pharmacol. Exp. Ther.* **199**, 336–352 (1976).

54. T. Sakaguchi, K. Arase, J. S. Fisler, G. A. Bray, Effect of starvation and food intake on sympathetic activity. *Am. J. Physiol.* **255**, R284–R288 (1988).

55. Y. Chen, T. V. Getchell, D. L. Sparks, M. L. Getchell, Patterns of adrenergic and peptidergic innervation in human olfactory mucosa: Age-related trends. *J. Comp. Neurol.* **334**, 104–116 (1993).

56. M. L. Getchell, T. V. Getchell, Fine structural aspects of secretion and extrinsic innervation in the olfactory mucosa. *Microsc. Res. Tech.* **23**, 111–127 (1992).

57. G. Vargas, M. T. Lucero, Dopamine modulates inwardly rectifying hyperpolarization-activated current (Ih) in cultured rat olfactory receptor neurons. *J. Neurophysiol.* **81**, 149–158 (1999).

58. Y. Okada, T. Miyamoto, K. Toda, Dopamine modulates a voltage-gated calcium channel in rat olfactory receptor neurons. *Brain Res.* **968**, 248–255 (2003).

59. M. Q. Nguyen, Z. Zhou, C. A. Marks, N. J. Ryba, L. Belluscio, Prominent roles for odorant receptor coding sequences in allelic exclusion. *Cell* **131**, 1009–1017 (2007).

60. N. L. Koster et al., Olfactory receptor neurons express D2 dopamine receptors. *J. Comp. Neurol.* **411**, 666–673 (1999).